Thermal Analysis and Management of Proton Exchange Membrane Fuel Cell Stacks for Automotive Vehicle

Lu Xing[a], Huawei Chang[b], Runqi Zhu[c], Ting Wang[b], Qifan Zou[b], Wentao Xiang[b], Zhengkai Tu[b,*]

[a] Mechanical and Construction Engineering, Northumbria University, Newcastle upon Tyne, NE1 8ST, United Kingdom

[b] School of Energy & Power Engineering, Huazhong University of Science & Technology, Wuhan, 430074, China

[c] China-EU Institute for Clean and Renewable Energy, Huazhong University of Science & Technology, Wuhan, 430074, China

*Corresponding author: tzklq@hust.edu.cn

Tel.: +86 (0) 15102756731

Abstract

The thermal management of a proton exchange membrane fuel cell (PEMFC) is crucial for fuel cell vehicles. This paper presents a new simulation model for the water-cooled PEMFC stacks for automotive vehicles and cooling systems. The cooling system model considers both the cooling of the stack and cooling of the compressed air through the intercooler. Theoretical analysis was carried out to calculate the heat dissipation requirements for the cooling system. The case study results show that more than 99.0% of heat dissipation requirement is for thermal management of the PEMFC stack; more than 98.5% of cooling water will be distributed to the stack cooling loop. It is also demonstrated that controlling cooling water flow rate and stack inlet cooling water temperature could effectively satisfy thermal management constraints. These thermal management constraints are differences in stack inlet and outlet cooling water temperature, stack temperature, fan power consumption, and pump power consumption.

Keywords: Automotive vehicle; Proton exchange membrane fuel cell; Cooling system; Thermal management

1 Introduction

A fuel cell converts chemical energy into electrical energy. The proton exchange membrane fuel cell (PEMFC), which uses hydrogen as fuel, has advantages such as low operating temperature, high energy conversion efficiency, and swift start-ups. At a low operating temperature, the PEMFC generates enough power (30-150kW) for the transport applications, such as vehicles, aerospace, mobile communications, railways locomotive, etc [1]. PEMFC can be the solution for low-emission vehicles in the future.

Despite higher efficiency than internal combustion engines, heat rejection from fuel cells remains challenging due to required lower operating temperatures. Meanwhile, heat dissipation through exhaust heat flow in typical vehicles is significantly reduced in the PEMFC vehicles. More than 95% of the waste heat is generated needs to be carried away by the refrigerant to maintain the fuel cell operating temperature. Temperature changes in PEMFC stacks are considerably higher during load variations, it is found to have a negative impact as they cause thermal stresses and stack material degradation. The PEMFC internal thermal balance plays a key role in efficiency optimization, fuel cell life span, and operational safety issues. Stack thermal management and control are, thus, crucial issues for the PEMFC vehicles [2,3].

Some research focus on investigating the single fuel cell of PEMFC, the thermal and water transport within and adjacent to the membrane-electrode assembly (MEA). Edwards and Demuren [4] used the CFD approach to develop an MEA model, incorporating water absorption/desorption resistances. Pourrahmani et al. [5] performed case studies to investigate the size effects of microporous layer (MPL) on convective heat transfer enhancement, the MPL is located in between the gas diffusion layer (GDL) and catalyst layer (CL). Sim et al. [6] studied the effect of ratio variation in the substrate and MPL on the performance of the fuel cell. Few researchers studied impacting factors on the performance of the PEMFC. Chugh et al. [7] developed a model for simulating the effects of operating variables such as temperature, pressure, and stoichiometry ratio on the PEMFC performance, the model had been validated against experimental results. Wang et al. [8] studied the effects of operating conditions on the PEMFC performance with anode recirculation. Mortada et al. [9] discussed the impact of the reactant flow nonuniformity on the performance. Some developed the thermal or water management modeling of the PEMFC stack. Zhao et al. [10] proposed a semi-empirical thermal management model for water-cooled PEMFC stacks, which they validated with experimental data of three different working conditions. Zhang et al. [11] predicted a PEMFC engine thermal management system performance using 1D and 3D integrating numerical simulation. Wang et al. [12] developed a data-driven model for simulating the PEMFC performance. This model demonstrated a comparable accuracy to the comprehensive 3D

physical model. Liso et al. [13] developed a model for a polymer electrolyte membrane's water mass balance in a PEMFC stack. Ou et al. [14] developed a multiple-input multiple-output fuzzy controller for controlling the humidity and temperature of the fuel cell. Zhang et al. [15] shows the pre-heating of the anode hydrogen is necessary for improving the durability of the PEMFC. Chen et al. [16] proposed an aging prognosis model which can predict the aging state of PEMFC, a water-cooling system controls the stack temperature. Sun et al. [17] researched the matching design method of a fuel cell's waste heat recovery system. Baroutaji et al. [18] discussed potential pathways for waste heat recovery of PEMFC.

Some worked on innovative cooling flow field design or cooling method to benefit the thermal or water management of the PEMFC stack. Ramezanizadeh et al. [19] carried out a comprehensive review of the fuel cells' cooling approaches. Ashrafi and Shams [20] modeled numerically the two-phase flow in the serpentine flow field, the best orientation with the lowest parasitic power is found. Ghasemi et al. [21] studied the effectiveness of applying six different cooling flow fields by simulation and shows typical serpentine has better performance than other models. Some researchers focus on novel cooling refrigerants implemented for the thermal management system [22,23]. Chen et al. [24] demonstrated that utilizing microencapsulated phase change suspension in a PEMFC reduces the required weight and volume of coolant and pump power consumption. Fly and Thring [25] made a comparison of evaporative and liquid cooling methods for fuel cell vehicles. Choi et al. [26] suggested that the two-phase HFE-7100 cooling method has an advantage in temperature maintenance and temperature uniformity over the single-phase water-cooling method. Bargal et al. [27] experimented with various nanofluids for thermal management of PEMFC stack.

There are research works which developed control strategies for thermal management and kept fuel cell in optimal operating conditions. Han et al. [28] investigated different control algorithms to maintain PEMFC stack temperatures for the vehicle. The radiator fan and three valves are operated to maintain the coolant inlet temperature. It is found that the model reference adaptive control, compared to the nominal feedback controller, is effective to address uncertainties and robust control due to the high inherent nonlinearity in the cooling systems. Han and Yu [29] investigated three driving conditions considering ram air compensation to evaluate the cooling system operating trajectory. While the vehicle is running, the external ram air entering the vehicle's frontal area helps to cool down the temperature of the fuel cell. This cooling air flow is the ram air and is critically important for the thermal management when the vehicle is operating. Xu et al. [30] developed a vehicle integrated thermal management system to control all components' temperatures within the required range. Yang et al. [31] developed a control-oriented model for a fuel cell thermal management system.

Research focuses on thermal and water management for the whole vehicle, such as forklift truck, bus, train or underwater vehicles. Hosseinzadeh et al. [32] developed a thermal and water management model of low-temperature PEMFC in forklift truck power systems. It suggests the humidifying of inlet air is quite important. Liso et al. [33] presented a control-oriented dynamic model of a liquid-cooled PEMFC for the forklift application. It studies temperature variations over fast load changes. The developed model approach can assist designers in choosing the required coolant mass flow rate and radiator size to minimize the stack temperature gradients. Cheng et al [34] proposed a model-based temperature regulation for controlling the thermal system of the PEMFC stack on a city bus. Cheng et al [35] also focused on the warm-up strategy on the city buses. A longer warm-up time and a higher environment temperature help improve efficiency. Jiang et al. [36] design a thermal management system for a fuel cell bus in a low-temperature environment. Peng et al. [37] suggested an offline optimal energy management strategy for a fuel cell hybrid train. Han et al. [38] developed a control strategy for the thermal management of the fuel cell system of a underwater vessel.

Improper temperature regulation could impact the durability of the PEMFC, some researchers investigated the impact of aging on fuel cell vehicle performance [39-43]. Oh et al. [44] proposed real-time fault detection and diagnosis method for the fuel cell. Yan et al. [45] developed a model-based fault-tolerant control for the system. Zhao et al. [46] proposed using a heat pump system to harvest the waste heat generated in a fuel cell vehicle. Lohse-Busch et al. [47] presented experimental data for the 2016 Toyota Mirai Fuel cell (FC) vehicle. The system efficiency, FC stack losses, FC system losses, etc were measured. Mayyas et al. [48] developed a 3D thermal model and control strategy for the 1.2kW PEMFC stack of the automotive powertrain. The thermoelectric module was integrated with the FC model.

In this paper, we developed a simulation model for the PEMFC stacks (30kW) for automotive vehicles and their cooling system. The model includes simulations and integrations of fuel cell stacks, intercooler, radiator, humidifier, fan, and water pump. The cooling system model considers the cooling of the stack and cooling of the compressed cathode intake air through the intercooler. By simulations, we calculated the heat dissipation requirements and heat dissipation (cooling system) capacity of the vehicle and the flow distribution of the stack cooling circuit and the intercooler cooling circuit. We also studied the dynamic characteristics of the heat dissipation capability of the heat dissipation system. Analyze the impact of variations of water flow rate and stack inlet cooling water temperature on the cooling system performance.

2 System description

Fig. 1 presents the schematic of the PEMFC systems on automotive vehicles. The system

is composed of a PEMFC stack, hydrogen tank, air compressor, intercooler, humidifier, and cooling system (water pump and radiator). Air is first compressed in the compressor; extreme high-temperature air will be cooled by the cooling water passing through the intercooler, humidified, then enter the cathode of the PEMFC stack. PEMFC stack-generated heat will also be taken away by cooling water. The stack operating temperature and cathode intake air temperature are regulated by controlling the stack inlet cooling water temperature and cooling water flow rate. The water pump distributes the low-temperature cooling water flows into the fuel cell stack and the intercooler through the three-way valve to remove the extra heat. The mixer mixed the high-temperature outlet cooling water exiting the intercooler and the PEMFC stack and flows through the radiator to exchange heat with the environment air. Then low-temperature radiator outlet cooling water will be distributed to the cooling loop again.

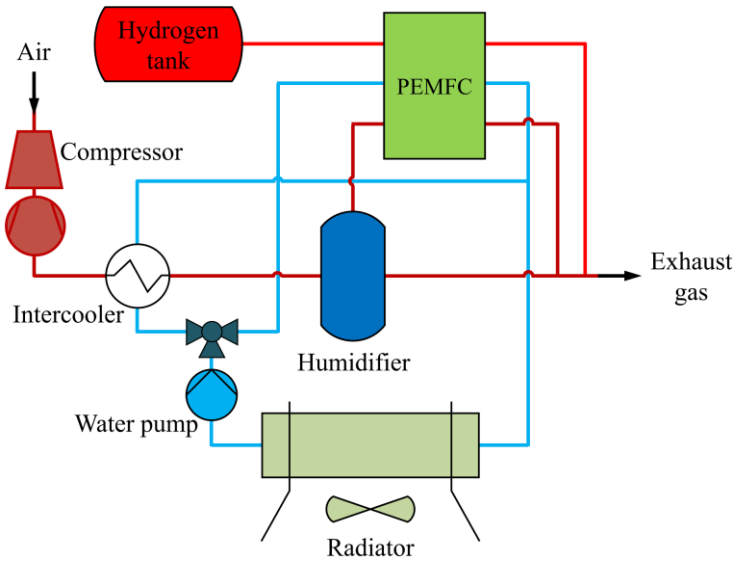

Figure 1: Schematic diagram of the whole system – PEMFC for automotive vehicles

3 System model and validation

It is critical to ensure the safe and stable operation of the PEMFC stack under different working conditions. We developed a simulation model to investigate whether it is sufficient to meet the heat dissipation requirements of the compressed cathode intake air and the PEMFC stack by controlling the cooling water flow rate and stack inlet cooling water temperature. Meanwhile, the PEMFC stack shall be operated at the optimal condition: (1) The single fuel cell operating voltage is typically set in the range of 0.60 ~ 0.75V when the energy conversion efficiency of the stack is within 50 % ~ 60 %. (2) Peak stack operating temperature shall be no higher than 363K, which otherwise results in Nafion conductivity loss and fuel cell performance degradation [49]. (3) Homogenization of stack temperatures distributions; it is preferred that the temperature difference of the stack inlet and outlet cooling water temperature is less than 10K, preferably less than 5K [7,50].

3.1 PEMFC stack model

The fuel cell stack is a core component of the PEMFC vehicle. It uses hydrogen as a fuel and oxygen as an oxidant, continuously outputs electrical energy through an electrochemical reaction. The output voltage of fuel cell can be obtained considering ohmic losses, concentration losses, and activation losses in the fuel cell stack, as shown in Equation (1):

$$V_{cell} = V_{Nernst} - V_{act} - V_{ohm} - V_{con} \quad (1)$$

Where, V_{cell} is the fuel cell voltage (V). V_{Nernst} is the Nernst open-circuit voltage (V) can be expressed as a function of fuel cell operating temperature, partial pressures of hydrogen and oxygen in the fuel cell, as presented in Equation (2). V_{act} is the activation voltage loss (V), which is the overpotential generated by the activation energy needed for overcoming the electrochemical reaction on the catalytic surface, as presented in Equation (3). V_{ohm} is the ohmic voltage loss (V) due to the impedance of transmission of electrons in the electrolyte and of the electrons in the conductive element, as presented in Equation (4). V_{con} is concentration loss (V), which is caused by a decrease in the concentration of the reactants in the electrochemical reaction, as presented in Equation (5). Empirical parameters in the modeling Equations (2) - (5) are for the fuel cell utilizing Nafion-212 membrane. The equations results have been validated using experimental results at or lower than 80°C operating temperature; more details of the validation will be described in section 3.6. The Nernst open-circuit voltage V_{Nernst} can be expressed in Equation (2) [51] as:

$$V_{Nernst} = 1.229 - 8.5 \times 10^{-4}(T_{st} - 298.15) + 4.308 \times 10^{-5} T_{st} (lnp_{H2} + 0.5 lnp_{O2}) \quad (2)$$

Where T_{st} is the PEMFC stack operating temperature (K); p_{H2} and p_{O2} are the partial pressures of hydrogen and oxygen (atm) in the fuel cell, respectively; p_{H2} and p_{O2} can be calculated as a function of T_{st}, cell current density I_{cell}/A etc using equations presented in [51]. A is the active cell area (cm^2). V_{act} can be expressed in Equation (3) [52] as:

$$V_{act} = -(\xi_1 + \xi_2 T_{st} + \xi_3 T_{st}(lnc_{O2}) + \xi_4 T_{st} ln\, I_{cell}) \quad (3)$$

The activation voltage loss is related to stack temperature T_{st} (K); concentration of the oxygen c_{O2} (mol/cm^3) and the current I_{cell} (A). The values for the empirical parameters are: $\xi_1 = -0.948$, $\xi_2 = 0.00304$, $\xi_3 = 7.6 \times 10^{-5}$ and $\xi_4 = -1.93 \times 10^{-4}$ [52]. The concentration of the oxygen c_{O2} is calculated as a function of stack temperature T_{st} (K) and partial pressure of the oxygen p_{O2} (atm) [53]. V_{ohm}can be expressed in Equation (4) [54] as:

$$V_{ohm} = I_{cell} \cdot \frac{\rho \cdot \tau_m}{A} \quad (4)$$

Where ρ is the membrane resistance (Ω·cm); τ_m is the thickness (cm) of the proton exchange membrane. The membrane resistance to proton conduction is the most dominant component [52, 54] for calculating the ohmic loss. Ohmic loss caused by electrode resistance and contacts resistance is not considered. The membrane resistance ρ, can be calculated as a

function of T_{st} (K), cell current density I_{cell}/A and membrane humidity λ (-) using equations presented in [54]. The membrane humidity λ is a function of the relative humidity of the inlet gas [7]. V_{con} can be expressed in Equation (5) [55] as:

$$V_{conc} = B\ln(1 - \frac{(I_{cell}/A)}{j_{max}}) \quad (5)$$

Where j_{max} is the maximum current density, 1.6A/cm^2; the empirical parameter $B = -0.016$ [55]. The PEMFC stack heat generation can be expressed as in Equation (6):

$$q_{st,heat} = N_{cell} \cdot (V_{Nernst} - V_{cell}) \cdot I_{cell} \quad (6)$$

Where, $q_{st,heat}$ is the PEMFC stack heat generation (W). N_{cell} is the number of fuel cells (-).

3.2 Stack cooling model

To simplify the model, we assume that the stack heat dissipation is entirely through the cooling system; other dissipation processes like exhaust gas or thermal radiation are ignored [34]. The PEMFC vehicle cooling system needs to be designed to meet the heat dissipation requirement for the PEMFC stack and the intercooler. The stack cooling model is developed to estimate the PEMFC stack's heat balance and estimate the fuel cell operating temperature. During various working conditions, the fuel cell operating temperature can be neither too low nor too high. Low stack operating temperature will result in a significant activation voltage loss in the stack and low power output. In contrast, high stack temperature will degrade the membrane and fuel cell performance.

To ensure the stack operating temperature is at a preferable range, generated heat in the fuel cell must be removed to cool the stack. There are mainly three methods of dissipating heat for the fuel cell vehicle: the heat taken away by the cooling water loop, the heat taken away by the exhaust gas generated in reaction, and the heat emitted by the fuel cell to the surrounding environment. Among these, the heat dissipated from the cooling water loop is dominant. Therefore, in the stack cooling model, it is assumed that the circulating water removes all the heat generated. Based on energy balance, the change of the stack temperature T_{st} (K) is determined by the heat generation $q_{st,heat}$ and heat dissipation of the fuel cell through the cooling water loop as shown in Equation (7):

$$C_{p,st}m_{st}\frac{dT_{st}}{dt} = q_{st,heat} - C_{p,water,st}\dot{m}_{water,st}(T_{water,out,st} - T_{water,in,st}) \quad (7)$$

Where, $C_{p,st}m_{st}$ is the thermal mass of the fuel cell stack (J/K). $C_{p,water,st}$ is the specific heat capacity of the cooling water (J/(kg·K)). $\dot{m}_{water,st}$ is the mass flow rate of the stack cooling water (kg/s); $T_{water,in,st}$ and $T_{water,out,st}$ are the stack inlet and stack outlet cooling water temperatures, respectively (K).

3.3 Air compressor model

Before entering the fuel cell cathode, the air needs to go through the air compressor to be compressed; the air temperature rises rapidly up to about 150 ℃. Hot air directly enters the stack will cause a decline in stack performance or even cause damage to the proton exchange membrane. The circulating cooling water passing through the intercooler will cool the high-pressure and high-temperature compressed air to the fuel cell operating temperature. The required air mass flow (kg/s) is $\dot{m}_{air,comp} = 3.57 \times 10^{-7} \lambda_c I_{cell} N_{cell}$. λ_c is the stoichiometry ratio of the air (-). The temperature after the air passes through the compressor $T_{air,out,comp}$ (K) is as shown in Equation (8):

$$T_{air,out,comp} = T_{air,in,comp} + \frac{T_{air,in,comp}}{\eta_c}\left[\left(\frac{p_{air,out,comp}}{p_{air,in,comp}}\right)^{\frac{\gamma_{air}-1}{\gamma_{air}}} - 1\right] \quad (8)$$

Where, $T_{air,in,comp}$ is the air inlet temperature (ambient temperature T_{atm}, K). γ_{air} is the adiabatic exponent, it is 1.4(-). η_c is the compressor efficiency (-). $p_{air,in,comp}$ and $p_{air,out,comp}$ are the inlet and outlet pressure (atm).

3.4 Intercooler cooling model and radiator model

The intercooler is used to cool the high-temperature and high-pressure compressor outlet air before it enters the cathode of the fuel cell stack. The intercooler (heat exchanger) is modeled using the Number of Transfer Unit (NTU) method. This method can calculate the maximum heat exchange between hot fluids (compressed air) and cold fluids (intercooler cooling water). The heat transfer rate of the intercooler heat exchanger $q_{intercooler,heat}$ (W) between the hot compressed air and cold intercooler cooling water can be calculated as Equation (9):

$$q_{intercooler,heat} = \varepsilon C_{min}(T_{hi} - T_{ci}) \quad (9)$$

Where, ε is effectiveness, the ratio between the actual heat transfer rate and the maximum possible heat transfer rate (-). C_{min} is the smaller one of $\dot{m}_{air} c_{p,air}$ and $\dot{m}_{water,inter} c_{p,water}$ (W/K). T_{hi} is the inlet temperature of the hot fluid exiting from the compressor, which equals to $T_{air,out,comp}$ (K) in Equation (8). T_{ci} is the inlet fluid temperature of cold fluid - intercooler cooling water (K). In the counterflow NTU heat exchanger, the effectiveness is calculated as $\varepsilon = \left(\frac{1-exp(-NTU(1+C))}{1+C}\right)$. $NTU = \frac{UA_{intercooler}}{\dot{C}_{min}}$ and $C = \frac{C_{min}}{C_{max}}$. U is the overall heat transfer coefficient (W/m^2·K). $A_{intercooler}$ is the heat transfer area of the intercooler (m^2). The radiator (heat exchanger) is also simulated using the NTU method.

3.5 Three-way valve and mixer model

The valve distributes part of the cooling water to the intercooler to cool the compressed

high-temperature air before it enters the fuel cell cathode; it circulates the rest of the cooling water to cool the PEMFC stack. The position of the valve determines the flow distribution. $\dot{m}_{water,st} = pos \cdot \dot{m}_{water,total}$ and $\dot{m}_{water,inter} = (1 - pos) \cdot \dot{m}_{water,total}$. $\dot{m}_{water,total}$ is the total cooling water flow rate (kg/s). When the position of the valve pos is 1, all circulating cooling water is distributed to cool the stack. When the position pos is 0, all circulating cooling water is distributed to the intercooler. The process of cooling water flowing through the valve is considered adiabatic.

The intercooler outlet cooling water and stack outlet cooling water are mixed at the mixer. The outlet mixer water temperature $T_{water,out,mix}$ (K) in the cooling loop can be calculated based on energy balance as $T_{water,out,mix} = \frac{\dot{m}_{water,st} T_{water,out,st} + \dot{m}_{water,inter} T_{water,out,inter}}{\dot{m}_{water,st} + \dot{m}_{water,inter}}$.

3.6 PEMFC model validation

Fig. 2 shows the single PEMFC fuel cell output voltage and heat generations at different operating temperatures 323K, 353K. The PEMFC employs the Nafion-212 membranes. As shown in Figure 2, when the fuel cell operates at different temperatures, the polarization curves are similar. When the current density increases to 1.2 A/cm^2, the single fuel cell voltage drops from about 1.0V to 0.4V; the heat generation increase quickly to about 50 W. When the PEMFC operating temperature increases from 323K to 353K, the same output current density will lead to the higher output voltage and lower fuel cell heat generation, which is preferred. The simulation results are compared to the experimental results [7]. At the operating temperature of 323K and 353K, the simulation results match the experimental results quite well, with a slight difference. The input parameters for the PEMFC model are listed in Table 1.

Table 1: Parameters of a single fuel cell for the experimental validation [7]

Parameter	Value	Units
Number of fuel cells N_{cell}	30	N/A
Operating temperature T_{st}	323, 353	K
Anode inlet gas pressure P_a	1.0	atm
Cathode inlet gas pressure P_c	1.0	atm
Current density I_{cell}/A	0-1.2	A/cm^2
Active area A	50	cm^2
Membrane thickness τ_m	0.00508	cm

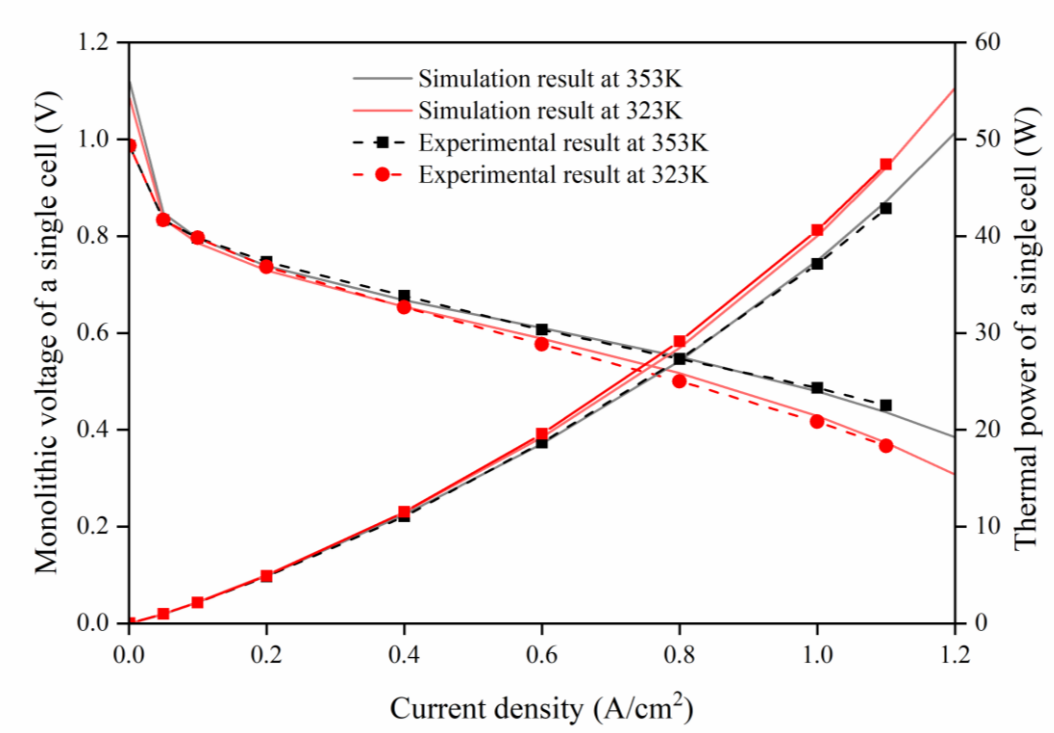

Figure 2: PEMFC output characteristic curve compared to experimental results [7]

4 System performance

Section 3 described a system model for estimating the performance of the PEMFC stack (for automotive vehicles) during various operating conditions. The model includes simulations and integrations of the PEMFC stack, stack cooling, air compressor, intercooler cooling, three-way valve, mixer, and radiator. The model calculates the fuel cell stack voltage, stack heat generation, it reveals the working mechanism of the fuel cell stack.

The PEMFC stack employs the Nafion-212 membranes. The performance of a single fuel cell has been validated against the experimental results using model parameters presented in Table 1 and equations shown in section 3.1. For applying fuel cell stack in the automotive vehicles, some parameters in Table 1, such as operating pressure, active area, etc., are re-adjusted. All stack model parameters used for the system performance evaluation are presented in Table 2. Based on the standard provided by the U.S. Department of Energy standard [49], the maximum operating temperature is set to be 90°C (363K). The parameters for the air compressor, intercooler, radiator, fan, and pump are presented in Table 3. Electric micro turbo (EMTC-150K) 5kW air compressor from Fischer Spindle has been chosen for the system simulation [56]. An electric fan and a water pump with an electric motor are used [57, 58].

Table 2: Parameters of the stack model used for the system performance evaluation

Parameter	Value	Units
Number of fuel cells N_{cell}	220 [1,35]	N/A
Stack maximum power $P_{sta,max}$	30 [1]	kW
Operating temperature T_{st}	320-360 [49]	K
Anode inlet gas pressure P_a	1.0	atm
Cathode inlet gas pressure P_c	1.6 [59]	atm
Anode stoichiometry λ_a	2.0 [7]	N/A
Cathode stoichiometry λ_c	2.0 [7]	N/A
Atmospheric temperature T_{atm}	298	K
Intake air temperature	348	K
Current density I_{cell}/A	0-1.2 [7]	A/cm^2
Active area A	260 [35]	cm^2

Table 3: Parameters of the air compressor, intercooler, radiator, fan, and pump

Parameter	Value	Units
Compressor air inlet temperature T_{atm}	298	K
Compressor efficiency η_c	0.75 [56]	N/A
Compressor inlet air pressure $p_{air,in,comp}$	1.0	atm
Compressor inlet air pressure $p_{air,out,comp}$	1.6	atm
Intercooler U value	50	W/(m^2·K)
Radiator U value	120 [60]	W/(m^2·K)
Fan efficiency	0.8	N/A
Pump efficiency	0.6 [57]	N/A

4.1 PEMFC operation condition

It is critical to ensure the safe and stable operation of the PEMFC stack under different working conditions. The single fuel cell operating voltage is usually set in the range of 0.60 ~ 0.75V when the energy conversion efficiency of the stack is within 50 % ~ 60 %; Stack operating temperature is preferred to be higher for higher fuel cell output power. However, the peak stack operating temperature shall be no higher than 363K. To maintain the PEMFC at optimal operation condition, the heat taken away by the cooling system needs to be promptly adjusted according to the stack heat generation and air compressor cooling demand. The cooling water flow rate required for the stack heat dissipation and air compressor cooling has been calculated.

4.2 Cooling system – intercooler and stack

In Fig. 1, partial cooling water circulates through the intercooler to take away the heat generated and stored in the compressed air. The rest of the cooling water circulates through the PEMC stack to dissipate the stack-generated heat. Assuming the stack inlet cooling water temperature is 343K, the stack operating temperature is 353K. As shown in Fig. 3 (a), when the current density increases, the heat dissipations through the intercooler is negligible and barely changes; the heat dissipation through the stack significantly increases. The heat dissipation ratio through the intercooler compared to the heat dissipation through the stack decreases from 0.6% to 0.5%. The cooling of the PEMFC stack determines more than 99.0% of the heat dissipation requirement.

Fig. 3 (b) presents the cooling water flow rate through the intercooler and through the stack. When the current density increases, the cooling water flow rate ratio through the intercooler compared to the one through the stack decreases from 1.2% to 0.9%. More than 98.5% of the cooling water is distributed to the PEMFC stack cooling loop. To simplify the system model, we can neglect the cooling water distributed to the intercooler and the heat dissipation through the intercooler.

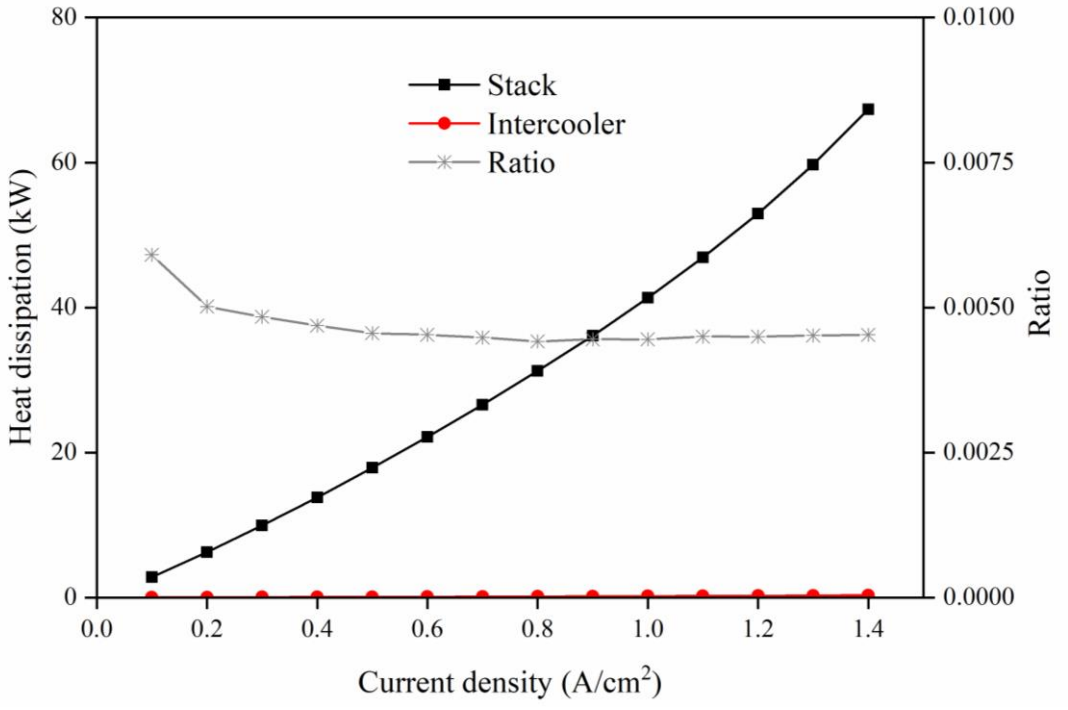

(a) Heat dissipation

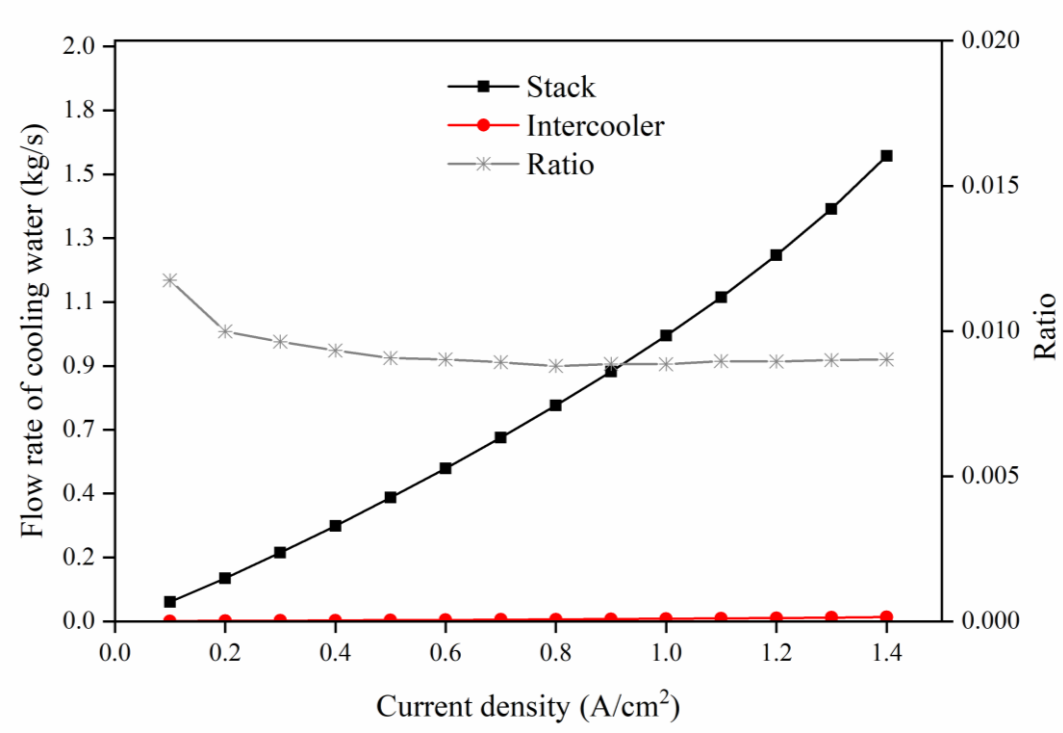

(b) cooling water flow rate

Figure 3: Heat dissipation and cooling water flow rate distribution (intercooler and stack)

4.3 Stack inlet and outlet cooling water temperature

Homogenization of temperature distributions is also required to ensure the safe and stable operation of the PEMFC stack under different working conditions. It is necessary that the temperature difference of the stack inlet and outlet cooling water temperature be less than 10K, preferably less than 5K. Fuel cell output current density impacts the temperature differences of stack inlet and outlet cooling water, as shown and discussed below. We also investigate how the stack cooling water flow rate and inlet cooling water temperature impact the differences.

4.3.1 Impact of stack cooling water flow rate

Fig. 4 (a) and (b) show the impact of the stack cooling water flow rate on stack outlet cooling water temperature and on the temperature difference. When the cooling water cooling rate increases from 1kg/s to 2kg/s, the stack outlet cooling water temperature, and the temperature difference decreases. In Fig. 4(a), when the flow rate is 1kg/s, the stack outlet cooling water temperature sometimes is higher than 363K. The maximum stack outlet water temperature shall not exceed 363K; the PEMFC shall not be operated under this condition. When the flow rate is 2kg/s, the stack outlet temperature is always lower than 363K. In Fig. 4(b), when the water flow rate is 2kg/s, the temperature difference is about 2K; when the water flow rate is 1kg/s, the temperature difference is about 4.5K. The difference between the stack inlet and outlet cooling water temperature is preferred to be less than 5K.

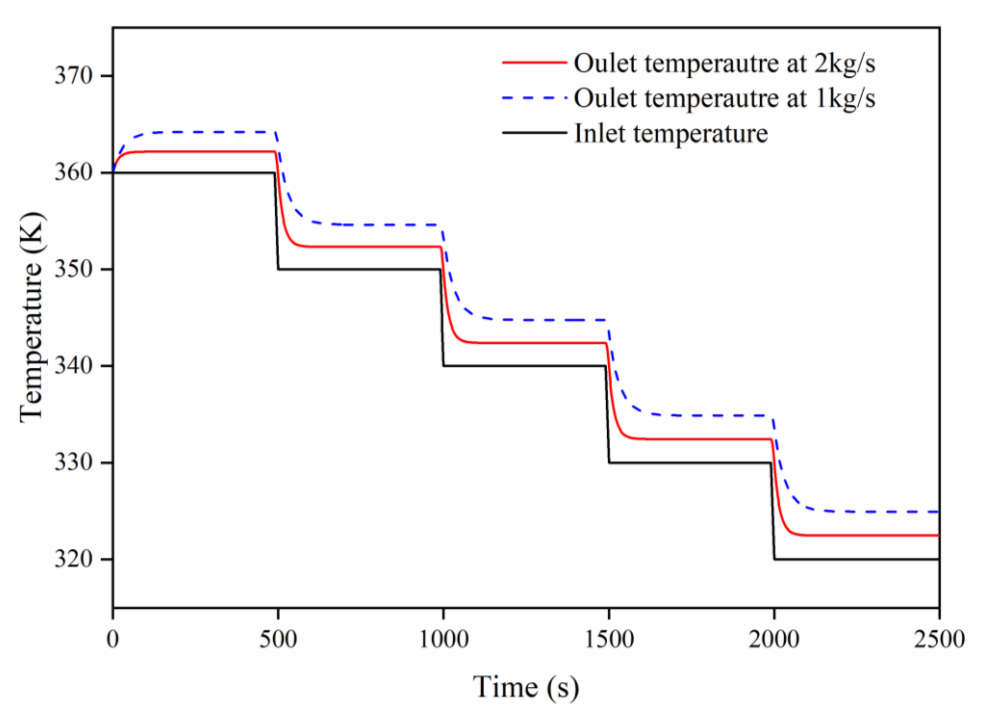

(a) PEMFC stack inlet and outlet cooling water temperature

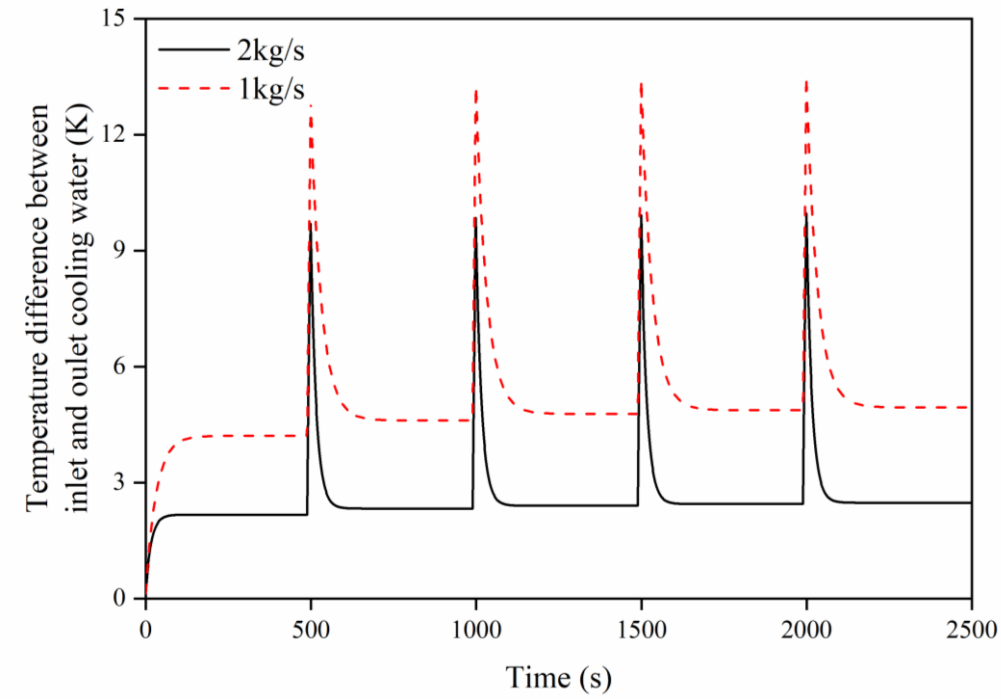

(b) difference of stack inlet and outlet cooling water temperature

Figure 4: Variations of cooling water flow rates (1kg/s and 2kg/s) impact on stack outlet cooling water temperature and temperature differences

In Fig. 4 (b), at the time 500s, there is a spike in the temperature difference result. This spike is a transient response to the change of stack inlet cooling water temperature. Sudden

change in the stack inlet cooling water temperature will lead to a spike in temperature difference, which is not preferred. The amplitude of the spike can be reduced by increasing the water flow rate. At a higher cooling water flow rate (2k/s), the response speed is also faster. When the flow rate is at 2kg/s, the response takes 48s before reaching a steady-state condition (within 0.1K); when the flow rate is at 1kg/s, the response time is 119s. For the system performance, a cooling water flow rate of 2kg/s is preferred, with advantages of a shorter response time, lower temperature difference, and better stability.

4.3.2 Impact of output current

Fig. 5 shows the impact of the output current (140A, 200A, and 260A) on the difference between stack inlet and outlet cooling water temperature. At the time of 0-500s, when the output current increases from 140A to 200A, the temperature difference increases from 2.8K to 4.2K. At the time 500s, the stack inlet water temperature is changed from 360K to 350K. The cooling system cannot quickly remove the heat generated in the stack; the temperature difference between the inlet and outlet cooling water appears to be significant. A sudden change in the stack inlet cooling water temperature causes a 10-14K spike in the results of temperature difference. This spike later decreases, and the temperature difference stabilizes. For the PEMFC stack applied for the automotive vehicles, the output current varies to adapt to the change of the car speed. It is less preferred to regulate the stack inlet cooling water temperature for meeting the increased heat dissipation requirement. Since it could lead to significant differences in the stack inlet and outlet cooling water temperature, this significant temperature difference could shorten the lifetime of the PEMFC stack.

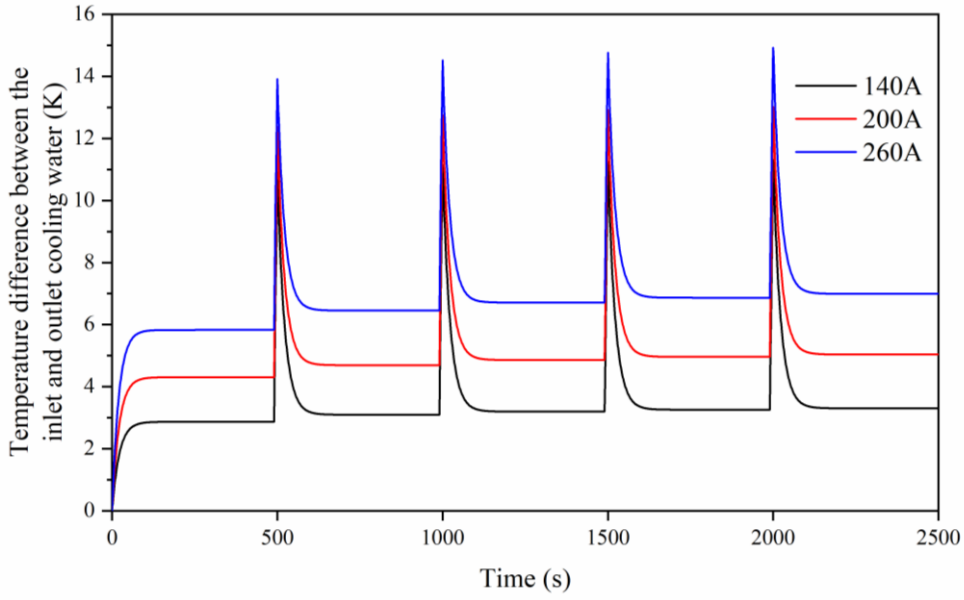

Figure 5: Variations of output current (60A, 100A, and 140A) impact on differences of stack inlet and outlet cooling water temperature

4.3.3 Impact of stack inlet cooling water temperature

Fig. 6 (a) and (b) present the impact of the stack inlet cooling water temperature on stack outlet cooling water temperature and the difference between stack inlet and outlet cooling water temperature. When the stack inlet cooling water temperature increases from 350K to 360K, the outlet temperature increases, and the temperature difference decreases. In Fig. 6(a), when the stack inlet cooling water temperature is 360K, the stack outlet cooling water temperature is always higher than 363K. It is preferred to operate the stack at a stack inlet temperature of 350K.

Fig. 6 (b) shows that when the stack inlet cooling water temperature is 350K, the temperature difference is more than 13K. If the cooling water flow rate increases from 0.5kg/s to 1.5kg/s, it can reduce the temperature difference to 5K. Continuous increasing the cooling water flow rate, its impact on the temperature difference results decreases. To meet the thermal management requirements, it is suggested first to regulate the cooling water flow rate.

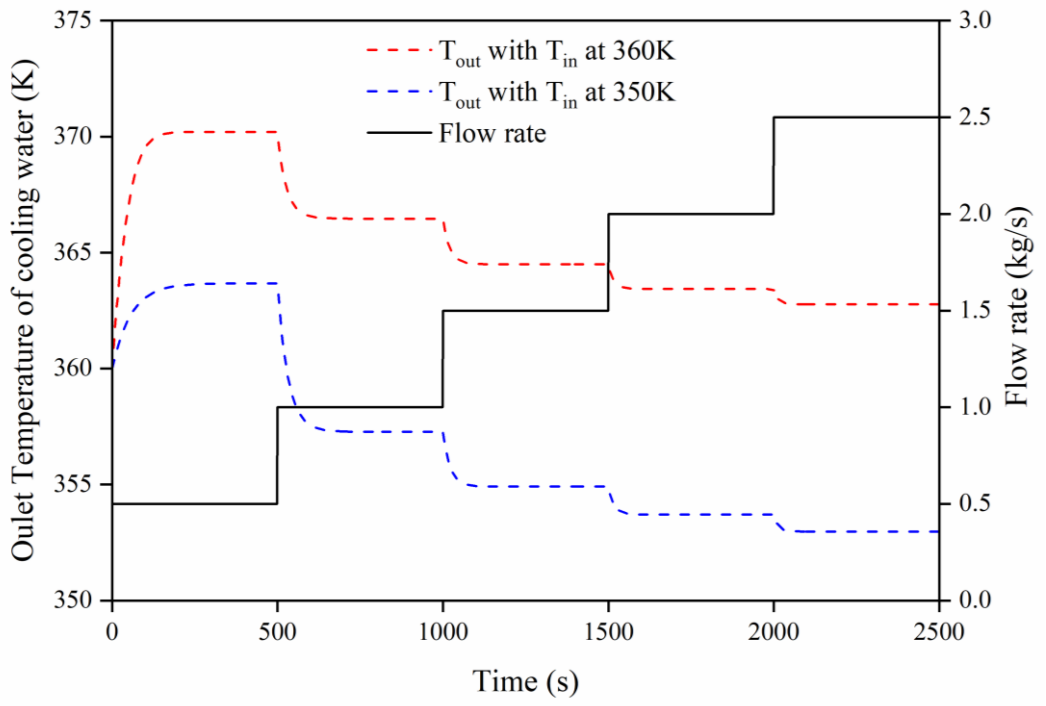

(a) PEMFC stack inlet and outlet cooling water temperature

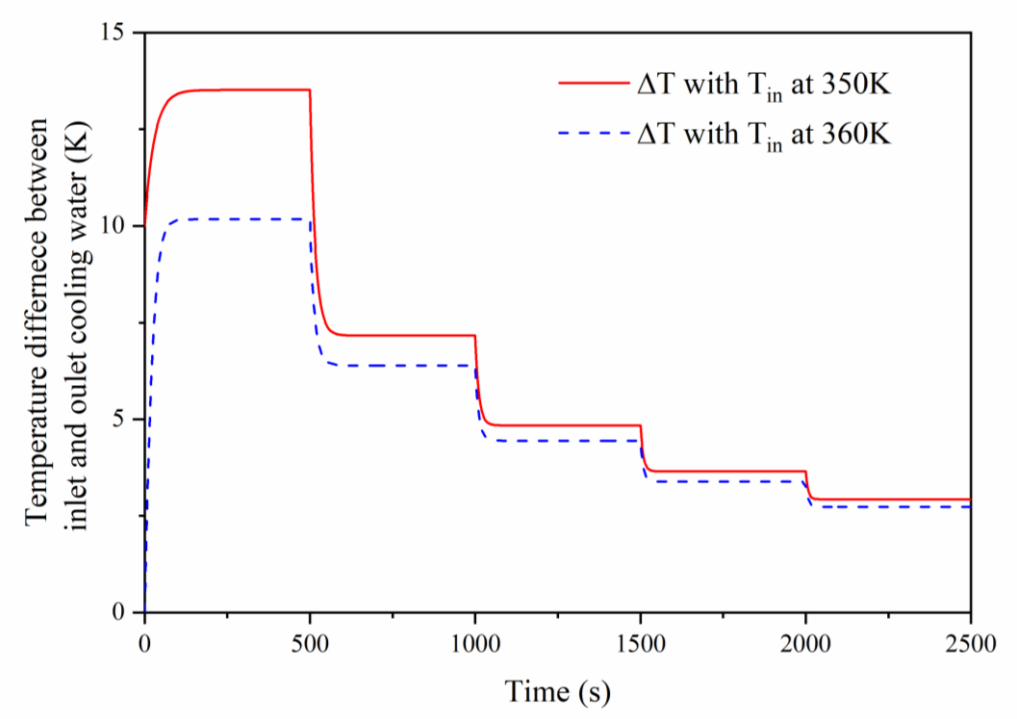

(b) difference of stack inlet and outlet cooling water temperature

Figure 6: Variations of stack inlet cooling water temperature (360K and 350K) impact on stack outlet cooling water temperature and temperature differences

4.4 Heat generation and dissipation of PEMFC stack

Fig. 7 (a) and (b) presents the stack heat generation and heat dissipation at the different stack inlet cooling water temperatures. In Fig. 7 (a), at a higher stack inlet cooling water temperature of 360K, the heat generation in the PEMFC is smaller, the heat dissipation requirement is reduced. Higher stack inlet cooling water temperature causes less stack heat generation. Every 500s, there is a step-change in the input cooling water flow rate, the flow rates change from 0.5kg/s to 1.0kg/s, 1.5kg/s, 2.0kg/s and 2.5kg/s. When the cooling water flow rate changes from 0.5kg/s to 2.5kg/s, stack heat generation increases, stack efficiency decreases. For fewer heat generations, a lower cooling water flow rate is preferred. There is a clear difference in the heat generation results at a very low flow rate (<1.5kg/s) and a flow rate higher than that. When the flow rate changes from 1.5kg/s to 2.5kg/s, there is less than 1kW difference in the stack heat generation result.

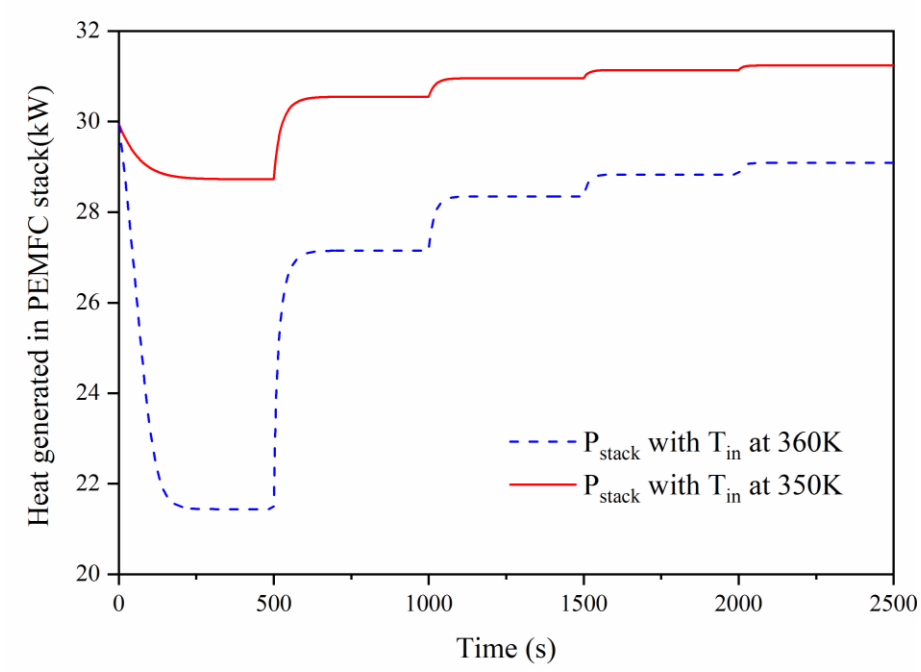

(a) PEMFC stack heat generation

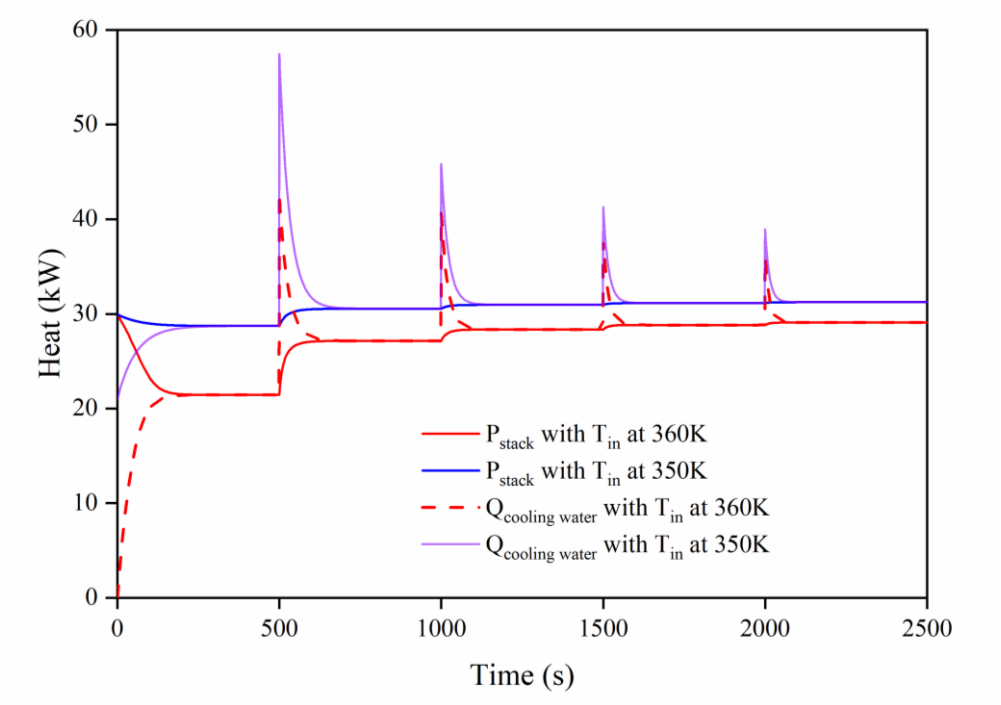

(b) Heat dissipation through the cooling system

Figure 7: Stack heat generation and heat dissipation at different stack inlet cooling water temperature (360K and 350K)

4.5 Water pump and fan power

The PEMFC stack produces power for the automotive vehicles; the water pump and the

fan consume power. The water pump and the fan are used for thermal management of the fuel cell stack. They are used for regulating the cooling water flow rate and stack inlet cooling water temperature to maintain the operating condition for the stack. Equations provided in Yu and Jung [57, 58] have been used for calculations of water pump and fan power consumption. Fig. 8 shows the fan and pump power changes with the cooling water flow rate. The cooling water flow rate changes from 1.0kg/s to 2.5kg/s, the water pump power consumption increases to 0.15 kW. At a higher stack temperature of 360K, the fan power consumption is lower. When the stack inlet cooling water temperature decreases from 360K to 350K, the fan power consumption at the steady state increase from 3kW to 6kW. To minimize the fan power and water pump power consumption, operating the fuel cell at a higher stack inlet cooling water temperature and a relatively smaller cooling water flow rate is suggested.

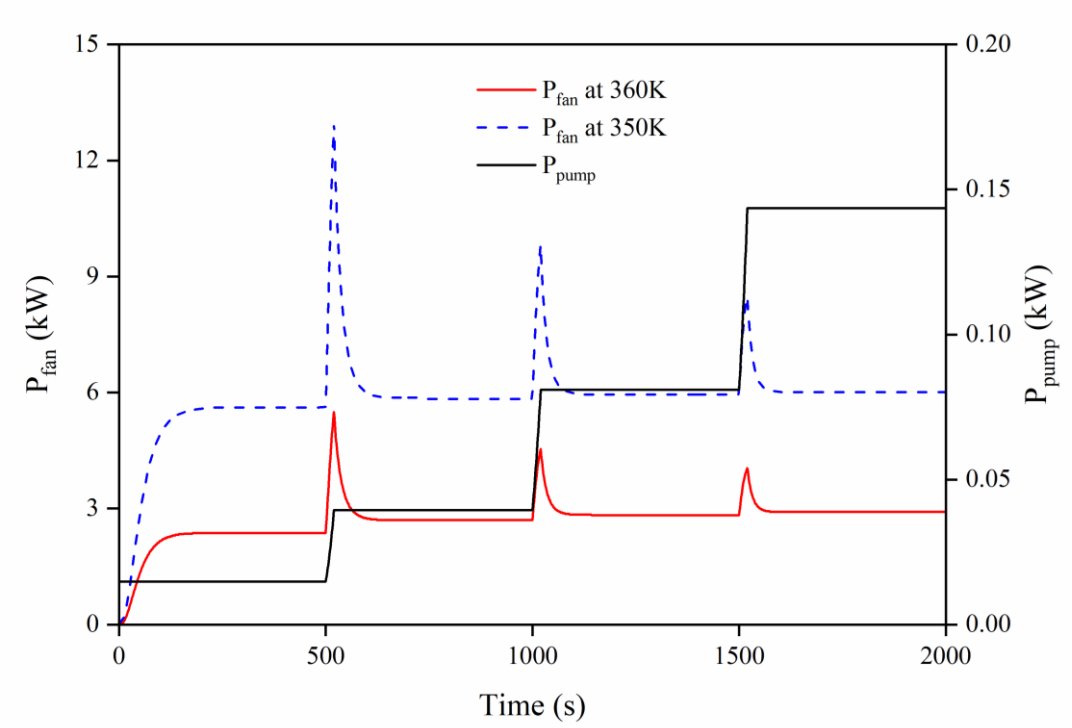

Figure 8: Fan and pump power varying with PEMFC stack cooling water flow rate

The energy efficiency $\eta_{net} = \frac{P_{net}}{P_{stack}}$ and net power $P_{net} = P_{stack} - P_{fan} - P_{pump}$ are calculated to evaluate fan and pump power ratio compared to stack output power at various stack operating conditions. The calculations quantify the impact of regulations of cooling water flow rate and stack inlet cooling water temperature on the stack energy performance. Controls of fan and water pump realize the regulations of the water flow rate and temperature. The energy consumption of the air compressor is not included in the calculations of P_{net}. In our study, the air is compressed to 1.6atm, the power consumption of the air compressor is constant (about 1.5kW) [50]. Fig. 9 presents the net output power P_{net} and energy efficiency η_{net} at the various stack inlet cooling water temperature, and different cooling water flow

rates. When the inlet temperature is 360K, and when the flow rate increases from 1.0kg/s to 2.5kg/s; the power consumption of the water pump increases, the energy efficiency decreases. The net output power decreases from 22kW to 21kW; efficiency decreases to 85%. When the flow rate is at 1kg/s, the inlet temperature increases from 340K to 360K; the net output power increases from 12kW to 22kW, efficiency increases from 50% to 85%. For higher net power and higher efficiency, less energy shall be consumed by the fan and the water pump. Higher stack inlet cooling temperature and lower cooling water flow rate are preferred.

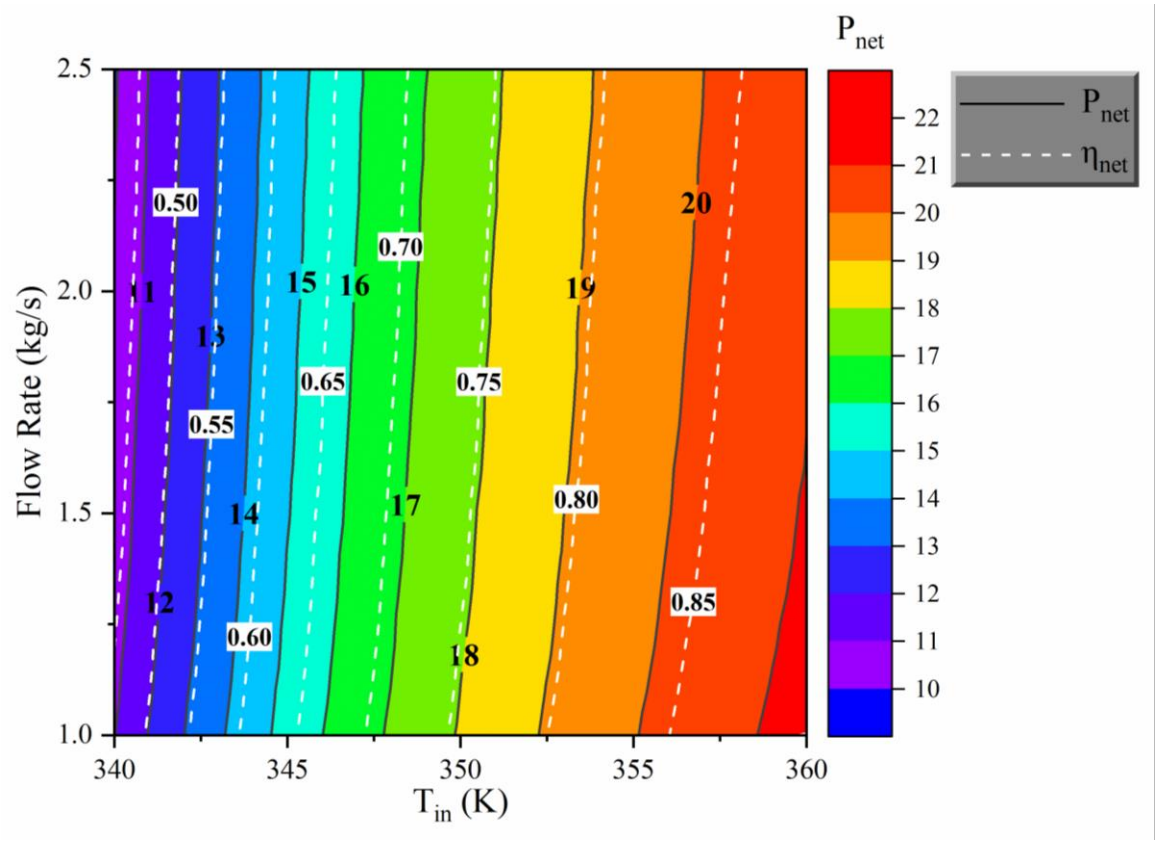

Figure 9: Net power output P_{net} and energy efficiency η_{net} at the various stack, inlet cooling water temperature and cooling water flow rate

In all, for the thermal management of the PEMFC stack for automotive vehicles, there are several constraints to be considered: such as differences in stack inlet and outlet cooling water temperature, stack temperature, fan power consumption, and pump power consumptions. Controls of the cooling water flow rate and stack inlet cooling water temperature help effectively satisfying these thermal management constraints. Based on the analysis results, to satisfy the stack heat dissipation needs during various operating conditions, we suggest maintaining the stack inlet cooling water temperature and moderating the cooling water flow rate. This control strategy allows the peak PEMFC stack temperature to be less than 363K. The stack inlet and outlet cooling water temperature differences are less than 5 K.

When the automotive vehicles speed up, more heat is generated in the PEMFC stack; the

required cooling water flow rate increases, the difference of stack inlet and outlet temperature decreases. The energy efficiency decreases, it is because the fan and the water pump consume more energy. When the required cooling water flow rate decreases, the energy efficiency increases, the difference of the stack inlet and outlet cooling water temperature increases. The rise in the temperature difference harms the life span of the fuel cell. We suggest that most of the time, the PEMFC stack be operated at high inlet cooling water temperature (350K-355K) and medium cooling water flow rate (1.5kg/s-2.0kg/s). Regulate the cooling water flow rate to meet the thermal management requirement; stack inlet cooling water temperature regulation is less preferred.

5 Conclusions

This paper presents a simulation model for the water-cooled PEMFC stacks for automotive vehicles and their cooling system. The cooling system model considers both the cooling of the stack and cooling of the inlet compressed air through the intercooler. Theoretical analysis has been carried out to calculate the heat dissipation requirements of the vehicle for the cooling system. The main conclusions for this case study are as follows:

- More than 99.0% of the heat dissipation requirement is for thermal management of the PEMFC stack; more than 98.5% of cooling water will be distributed to the PEMFC stack cooling loop for meeting the heat dissipation requirement. The rest of the cooling water will be distributed to cool the compressed high-temperature air before entering the cathode. To simplify the system model, we can neglect the cooling water distributed to the intercooler and the heat dissipation through the intercooler.
- Controlling the cooling water flow rate and stack inlet cooling water temperature could effectively satisfy the thermal management constraints. These constraints are differences in stack inlet cooling water temperature, outlet cooling water temperature, stack operating temperature, fan, and pump power consumption. The cooling water flow rate and stack inlet cooling water temperature are controlled by operating the fan and water pump.
- It is preferred the PEMFC stack mainly operates at constant and high inlet cooling water temperature (350K-355K) and medium cooling water flow rate (1.5kg/s-2.0kg/s). To meet the thermal management requirements, it is suggested first to regulate the cooling water flow rate.
- When the required cooling water flow rate increases, stack inlet and outlet cooling temperature differences decrease. Energy efficiency decreases because fan and water pump power consumption increases. When the required flow rate decreases, energy efficiency increases. The rise in the difference between the stack inlet and outlet cooling temperature might harm the life span of the fuel cell.

Acknowledgments

This work was supported by the National Key Research and Development Program of China (No.2018YFC0810000), the National Natural Science Foundation of China (No. 51776144), Natural Science Foundation of Hubei Province (No. 2020CFA040).

References

[1] Wang Y, Seo BJ, Wang BW, Zamel N, Jiao K, Adroher XC. Fundamentals, materials, and machine learning of polymer electrolyte membrane fuel cell technology. Energy and AI. 2020; 1: 100014.

[2] Gao JW, Li M, Hu YF, Chen H and Ma Y. Challenges and developments of automotive fuel cell hybrid power system and control. Science China Information Sciences 2019; 62(5): 1-25.

[3] Chen Q, Zhang GB, Zhang XZ, Sun C, Jiao K and Wang Y. Thermal management of polymer electrolyte membrane fuel cells: A review of cooling methods, material properties, and durability. Applied Energy 2021; 286.

[4] Edwards R and Demuren A. Interface model of PEM fuel cell membrane steady-state behavior. International Journal of Energy and Environmental Engineering 2019; 10 (1): 85-106.

[5] Pourrahmani H, Moghimi M and Siavashi M. Thermal management in PEMFCs: The respective effects of porous media in the gas flow channel. International Journal of Hydrogen Energy 2019; 44(5):3121-3137.

[6] Sim JB, Kang M, Min K. Effects of ratio variation in substrate and micro porous layer penetration on polymer exchange membrane fuel cell performance. International Journal of Hydrogen Energy 2021, 46(35):18615-18629.

[7] Chugh S, Chaudhari C, Sonkar K, Sharma A, Kapur G, Ramakumar S. Experimental and modeling studies of low temperature PEMFC performance. International Journal of Hydrogen Energy. 2020; 45: 8866-74.

[8] Wang BW, Wu KC, Xi FQ, Xuan J, Xie X, Wang XY, Jiao K. Numerical analysis of operating conditions effects on PEMFC with anode recirculation. 2019; 173: 844-856.

[9] Mortada M, Ramadan HS, Faraj J, Faraj A, Hage HE, Khaled M. Impacts of reactant flow nonuniformity on fuel cell performance and scaling-up: Comprehensive review, critical analysis and potential recommendations. International Journal of Hydrogen Energy 2020.

[10] Zhao XQ, Li YK, Liu ZX, Li Q and Chen QR. Thermal management system modeling of a water-cooled proton exchange membrane fuel cell. International Journal of Hydrogen Energy 2015; 40(7): 3048-3056.

[11] Zhang QG, Xu LF, Li JQ and Ouyang MG. Performance prediction of proton

exchange membrane fuel cell engine thermal management system using 1D and 3D integrating numerical simulation. International Journal of Hydrogen Energy 2018; 43: 1736-1748.

[12] Wang BW, Zhang GB, Wang HZ, Xuan J, Jiao K. Multi-physics-resolved digital twin of proton exchange membrane fuel cells with a data-driven surrogate model. Energy and AI. 2020; 1: 100004.

[13] Liso V, Araya SS, Olesen AC, Nielsen MP, Kær SK. Modeling and experimental validation of water mass balance in a PEM fuel cell stack. International Journal of Hydrogen Energy 2016, 41(4):3079-3092.

[14] Ou K, Yuan WW, Choi M, Yang SG, Kim YB. Performance increase for an open-cathode PEM fuel cell with humidity and temperature control. International Journal of Hydrogen Energy 2017, 42(50):29852-29862.

[15] Zhang QG, Tong ZM, Tong SG, Cheng ZW. Research on low-temperature heat exchange performance of hydrogen preheating system for PEMFC engine, International Journal of Hydrogen Energy 2020, 45(55):30966-30979.

[16] Chen K, Laghrouche S, Djerdir A. Aging prognosis model of proton exchange membrane fuel cell in different operating conditions. International Journal of Hydrogen Energy 2020, 45(20):11761-11772.

[17] Sun W, Yi FY, Hu DH and Zhou JM. Research on matching design method of waste heat reuse system of fuel cell vehicle considering system energy consumption and waste heat exchange rate. Internal Journal of Energy Research 2021; 45(4): 5470-5485.

[18] Baroutaji A, Arjunan A, Ramadan M, Robinson J, Alaswad A, Abdelkareem MA and Olabi AG. Advancements and prospects of thermal management and waste heat recovery of PEMFC. International Journal of Thermofluids 2021; 9.

[19] Ramezanizadeh M, Nazari MA, Ahmadi MH, Chen LG. A review on the approaches applied for cooling fuel cells. International Journal of Heat and Mass Transfer 2019,139:517-525.

[20] Ashrafi M and Shams M. The effects of flow-field orientation on water management in PEM fuel cells with serpentine channels. Applied Energy 2017; 208: 1083-1096.

[21] Ghasemi M. Ramiar A, Ranjbar AA and Rahgoshay SM. A numerical study on thermal analysis and cooling flow fields effect on PEMFC performance. International Journal of Hydrogen Energy 2017; 42(38): 24319-24337.

[22] Zhang GS and Kandlikar SG. A critical review of cooling techniques in proton exchange membrane fuel cell stacks. International Journal of Hydrogen Energy 2012; 37(3): 2412-2429.

[23] Bargal MHS, Abdelkareem MAA, Tao Q, Li J, Shi JP and Wang YP. Liquid cooling

techniques in proton exchange membrane fuel cell stacks: A detailed survey. Alexandria Engineering Journal 2020; 59: 635-655.

[24] Chen ST, Wang XK, Li WW, Wang SB, et al. Experimental study on cooling performance of microencapsulated phase change suspension in a PEMFC. International Journal of Hydrogen Energy 2017; 42(50): 30004-30012.

[25] Fly A and Thring RH. A comparison of evaporative and liquid cooling methods for fuel cell vehicles. International Journal of Hydrogen Energy 2016; 41(32):14217-14229.

[26] Choi EJ, Park JY and Km MS. A comparison of temperature distribution in PEMFC with single-phase water cooling and two-phase HFE-7100 cooling methods by numerical study. International Journal of Hydrogen Energy 2018; 43(29): 13406-13419.

[27] Bargal MHS, Souby MM, Abdelkareem MAA, Sayed M et al. Experimental investigation of the thermal performance of a radiator using various nanofluids for automotive PEMFC applications. Energy Research 2020.

[28] Han JY, Yu SS and Yi S. Advanced thermal management of automotive fuel cells using a model reference adaptive control algorithm. International Journal of Hydrogen Energy 2017; 42(7): 4328-4341.

[29] Han JY and Yu SS. Ram air compensation analysis of fuel cell vehicle cooling system under driving modes. Applied Thermal Engineering 2018; 530-542.

[30] Xu JM, Zhang CZ, Fan RJ, Bao HH et al. Modelling and control of vehicle integrated thermal management system of PEM fuel cell vehicle. Energy 2020; 199:117495.

[31] Yang LR, Karnik A, Pence BJ, Waez MTB and Ozay N. Fuel cell thermal management: modeling, specifications, and correct-by-construction control synthesis. IEEE Transactions on Control Systems Technology 2020;28(5):1638-1651.

[32] Hosseinzadeh E, Rokni M, Rabbani A and Mortensen HH. Thermal and water management of low temperature Proton Exchange Membrane Fuel Cell in fork-lift truck power system. Applied Energy 2013; 104: 434-444.

[33] Liso V, Nielsen MP, Koer SK and Mortensen HH. Thermal modeling and temperature control of a PEM fuel cell system for forklift applications. International Journal of Hydrogen Energy 2014; 39: 8410-8420.

[34] Cheng SL, Fang C, Xu LF, Li JQ, Ouyang MG. Model-based temperature regulation of a PEM fuel cell system on a city bus. International Journal of Hydrogen Energy. 2015; 40: 13566-13575.

[35] Cheng SL, Xu LF, Wu K, Fang C et al. Optimal warm-up control strategy of the PEMFC system on a city bus aimed at improving efficiency. International Journal of Hydrogen Energy 2017; 42: 11632-11643.

[36] Jiang HL, Xu LF, Li JQ, Hu ZY and Ouyang MG. Design and control of thermal

management system for the fuel cell vehicle in low-temperature environment. SAE Technical Paper 2020.

[37] Peng HJ, Chen Z, Li JX, Deng K, Dirkes S, et al. Offline optimal energy management strategies considering high dynamics in batteries and constraints on fuel cell system power rate: From analytical derivation to validation on test bench. Applied Energy 2021, 282(A):116152.

[38] Han JY, Han J, Ji HJ, Yu SS. “Model-based” design of thermal management system of a fuel cell “air-independent” propulsion system for underwater shipboard. International Journal of Hydrogen Energy 2020, 45(56):32449-32463.

[39] Kandidayeni M, Macias A, Boulon L and Kelouwani S. Investigating the impact of aging and thermal management of a fuel cell system on energy management strategies. Applied Energy 2020; 274: 115293.

[40] Song K, Ding YH, Hu X, Xu HJ, Wang YM, Cao J. Degradation adaptive energy management strategy using fuel cell state-of-health for fuel economy improvement of hybrid electric vehicle. Applied Energy 2021, 285(1):116413.

[41] Yue ML, Masry ZA, Jemei S, Zerhouni N. An online prognostics-based health management strategy for fuel cell hybrid electric vehicles. International Journal of Hydrogen Energy 2021, 46(24): 13206-13218.

[42] Han J, Han J, Yu S. Investigation of FCVs durability under driving cycles using a model-based approach. Journal of Energy Storage 2020, 27:101169.

[43] Kong S, Bressel M, Hilairet M, Roche R. Advanced passivity-based, aging-tolerant control fro a fuel cell/super-capacitor hybrid system. Control Engineering Practice 2020, 105: 104636.

[44] Oh HY, Lee WY, Won JY, Kim MJ, et al. Residual-based fault diagnosis for thermal management systems of proton exchange membrane fuel cells. Applied Energy 2020; 277: 115568.

[45] Yan CZ, Chen J, Liu H and Lu HX. Model-based fault tolerant control for the thermal management of PEMFC systems. IEEE Transactions on Industrial Electronics 2020; 67(4): 2875-2884.

[46] Zhao Z, Wang T, Zhang BF, Wang YQ, Bao CJ, Ji ZY. Analysis of an integrated thermal management system with a heat-pump in a fuel cell vehicle. AIP Advances 2021, 11: 065307.

[47] Lohse-Busch H, Stutenberg K, Duoba M, Liu XY, Elgowainy A, Wang M, et al. Automotive fuel cell stack and system efficiency and fuel consumption based on vehicle testing on a chassis dynamometer at minus 18°C to positive 35°C temperatures. International Journal of Hydrogen Energy. 2020; 45; 861-872.

[48] Mayyas AR, Ramani D, Kannan AM, Hsu K, Mayyas A, Schwenn T. Cooling strategy for effective automotive power trains: 3D thermal modeling and multi-faceted approach for integrating thermoelectric modules into proton exchange membrane fuel cell stack. International Journal of Hydrogen Energy. 2014; 39 (30): 13327-17335.

[49] The US Department of Energy (DOE). Energy Efficiency and Renewable Energy http://www.eere.energy.gov/hydrogenandfuelcells/mypp/pdfs/fuel_cells.pdf and the US DRIVE Fuel Cell Technical Team Technology Roadmap (revised 25 January 2012) http://www.uscar.org/guest/teams/17/Fuel-Cell-Tech-Team.

[50] Kang SG, Min KD, Mueller F, Brouwer J. Configuration effects of air, fuel, and coolant inlets on the performance of a proton exchange membrane fuel cell for automotive applications. International Journal of Hydrogen Energy. 2009; 34: 6749-6764.

[51] Chakraborty UK, Abbott TE, Das SK. PEM fuel cell modeling using differential evolution. Energy. 2012; 40:387-99.

[52] Mann RF, Amphlett JC, Hooper MAI, Jensen HM et al. Development and application of a generalized steady-state electrochemical model for a PEM fuel cell. Journal of Power Sources 2000; 86: 173-180.

[53] Amphlett JC, Baumert RM, Mann RF, Peppley BA, Roberge PR, Harris TJ. Performance modeling of the Ballard Mark IV solid polymer electrolyte fuel cell: I. Mechanistic model development. Journal of the Electrochemical Society. 1995;142:1.

[54] Khan M, Iqbal M. Modelling and analysis of electrochemical, thermal, and reactant flow dynamics for a PEM fuel cell system. Fuel cells. 2005;5:463-75.

[55] Jia J, Li Q, Wang Y, Cham Y, Han M. Modeling and dynamic characteristic simulation of a proton exchange membrane fuel cell. IEEE Transactions on Energy Conversion. 2009;24:283-91.

[56] Li YH, Pei PC, Ma Z, Ren P, Huang H. Analysis of air compressor, progress of compressor and control for optimal energy efficiency in proton exchange membrane fuel cell. Renewable and Sustainable Energy Reviews. 2020; 113: 110304.

[57] Yu SS and Jung DH. Thermal management strategy for a proton exchange membrane fuel cell system with a large active cell area. Renewable Energy 2008; 33:2540-2548.

[58] Yu SS and Jung DH. A study of operation strategy of cooling module with dynamic fuel cell system model for transportation application. Renewable Energy 2010; 35: 2525-2532.

[59] Qin YZ, Du Q, Fan MZ, Chang YF, Yin Y. Study on the operating pressure effect on the performance of a proton exchange membrane fuel cell power system. Energy Conservation and Management. 2017; 142: 357-365.

[60] Canli E, Darici S, Dogan S, Ozgoren M. Experimental performance analysis of

finned in line circular tube bank intercooler configuration at low range thermal capacity ratios. International Scientific Conference (Unitech11) Bulgaria. 2011; 377-82.